MOLECULAR PHYSICS, 1995, VOL. 86, NO. 5, 1099–1121

Molecular orientational motion in PCH5: computer simulations and models

By S. YE. YAKOVENKO, A. A. MURAVSKI
Institute of Applied Physics Problems, Kurchatova 7, Minsk, 220064, Republic of Belarus

G. KRÖMER and A. GEIGER
Institute of Physical Chemistry, Dortmund University, Otto-Hahn-Strasse, D-44221 Dortmund, Germany

(*Received 25 April 1995; revised version accepted 6 June 1995*)

The tumbling molecular motion in mesomorphic systems in discussed, based on a molecular dynamics computer simulation of a typical mesogen PCH5 within the united atom approach. It is shown that conformational molecular flexibility plays an important role not only in the orientational distribution of the molecules in the mesophase, but also in their dynamics. Being subjected to strongly fluctuating intermolecular forces, the relative position of the atoms in the molecule exhibit relaxation in the same time-scale as the intermolecular torque, which is much shorter than expected from the corresponding molecular moments of inertia. This results in a very fast short-time decay of the re-orientational autocorrelation functions of the molecule fragments. In spite of this rather complicated picture, cage models can be used to fit the re-orientational autocorrelation functions. For a more precise fit to the experimental functions one has to account for the real distribution function of the cage potential curvature.

1. Introduction

Since the first studies of molecular rotation in liquid crystals [1], there has been a lasting interest in this field. It is established now [2] that the re-orientation of the molecules in the mesophase can be described well by orientational diffusion models for motions in media with partial translational and orientational order (see Chapter 3 in [2] and references therein). This enables a fairly good interpretation of spectroscopic data obtained by NMR, ESR, steady state and time resolved polarized fluorescence, dielectric relaxation, and vibrational band-shape measurements (see corresponding chapters in [2]). Recently, femtosecond spectroscopy has provided some evidence for the existence of some fast motions in substances consisting of molecules similar to mesogens [3, 4]. The same feature was observed for mesogens themselves [5]. Experimental studies of different optical properties with both time resolved [3, 4] and steady state [5] methods revealed the orientational nature of these movements, and encouraged more detailed studies in this field.

We use the method of molecular dynamics computer simulations [6], a technique which provides the time evolution of the system explicitly. We have reported such a study for a typical mesogen *p*-n-pentyl-(*p'*-cyanophenyl)cyclohexane (PCH5) [7] and showed that computer simulations enable a detailed prediction of the molecular properties of real mesogens even for small mesogenic systems. In this paper we use

0026-8976 95 $10.00

this method to study the origin of the femtosecond relaxation of the orientational autocorrelation functions (CFs) of mesogens. We use PCH5 as typically representative of this kind of substance, but an extension of our conclusions is straightforward.

More generally, our work aims to find more appropriate models than the diffusional ones, to describe molecular re-orientation in the whole time interval available from contemporary experimental methods.

2. Simulations

Simulation data for PCH5 were obtained by the molecular dynamics method with 50 and 100 molecules in a box with periodic boundary conditions using the general simulation program package GROMOS [8]. For the simulation, the molecule (1) was divided into 18 fragments ('pseudoatoms', CH_n, $n = 0, 1, 2, 3$) and the nitrogen atom. The intra- and intermolecular interaction parameters were taken from GROMOS, except for the charges of the cyano fragment which were $0{\cdot}28e$ from the parameter set of GROMOS [8], or $0{\cdot}5e$ [9]. Details of the simulation procedure, interaction potential and the treatment of the simulation data can be found in [10]. Several systems with different numbers of molecules and different partial charges have been simulated. Their main features and the notation used hereafter are summarized in table 1. Both the isotropic and nematic phases were simulated at the same temperature, 333 K, just above the transition temperature of the real substance. The exact transition temperature of the model system is not known, but no drift of the order parameters towards the phase transition was observed. This is an obvious

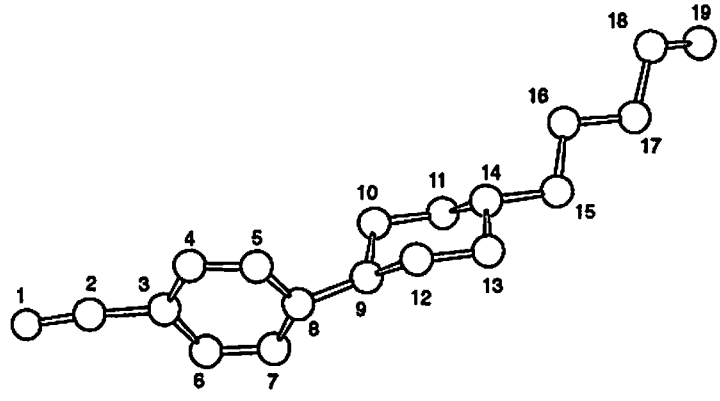

Structure 1

Table 1. The main parameters of the simulated ensembles.

Notation	Phase	Number of molecules	Partial charges of the cyano group	$\langle P_2 \rangle$
Iso	isotropic	50	$0{\cdot}50e$	0·216
Rigd	isotropic	50	$0{\cdot}50e$	0·215
Nem1	nematic	100	$0{\cdot}50e$	0·706
Nem2	nematic	100	$0{\cdot}28e$	0·687
Nem3	nematic	50	$0{\cdot}50e$	0·640

indication of the limited size of the simulation box in treating macroscopic properties but, as has been shown in [7], this only has a minor effect on the local properties, and even the correct values of various order parameters can be obtained from the simulation data after re-scaling.

3. Results and discussion

Before starting to discuss the results derived from the molecular dynamics simulations, some remarks should be made about different definitions of the rotating molecular frame. From the theoretical point of view it is natural to connect the axes of the intrinsic molecular system with the principal axes of the molecular moment of inertia ellipsoid. However, probably its movement can be observed only in neutron scattering experiments. Using optical or spectroscopic methods, one is restricted to the motion of some part of the molecule. In infrared or Raman spectroscopy one observes some characteristic band, the corresponding mode comprising only a few atoms as for cyano or benzene ring vibrations [7, 11]. In luminescence spectra [5, 12] only the dynamics of the chromophore is observable. Even in time resolved optical Kerr effect experiments [3, 4], where a grating of the refractive index is induced, one cannot observe the overall motion of the molecules; only conjugated bonds contribute to the molecular polarizability anisotropy which are responsible for this effect. Therefore here we shall talk about the motion of different molecular fragments as well as about the motion of the molecule as a whole.

3.1. *Basic definitions and properties*

Orientational autocorrelation functions of the form

$$C_{Lm}(\tau) = \langle \Phi_{Lm}(t, \tau)/\Xi_{Lm}(t, \tau)\rangle_t, \tag{1}$$

where

$$\Phi_{Lm}(t, \tau) = \langle D^L_{m0}[\Omega(t)]\, D^{L*}_{m0}[\Omega(t+\tau)]\rangle_{\mathrm{mol}} - \langle D^L_{m0}[\Omega(t)]\rangle_{\mathrm{mol}} \langle D^{L*}_{m0}[\Omega(t+\tau)]\rangle_{\mathrm{mol}},$$

$$\Xi_{Lm}(t, \tau) = [\langle |D^L_{m0}[\Omega(t)]|^2 - |\langle D^L_{m0}[\Omega(t)]\rangle_{\mathrm{mol}}|^2\rangle_{\mathrm{mol}} \times \langle |D^L_{m0}[\Omega(t+\tau)]|^2 - \langle D^L_{m0}[\Omega(t+\tau)]\rangle_{\mathrm{mol}}|^2\rangle_{\mathrm{mol}}]^{1/2},$$

have been computed from the simulated molecular configurations. $D^L_{m0}(\Omega(t))$ are Wigner rotation functions of a set of Euler angles determining the molecular orientation at time t in the principal axes frame of the order parameter tensor of the simulated system. $\langle \cdots \rangle_t$ and $\langle \cdots \rangle_{\mathrm{mol}}$ denote averaging over the time and the molecules in the system, respectively. Subtraction of the average values enabled comparison between different phases and different fragments. For example, for long simulation runs in the isotropic phase $C_{20}(t) + 2C_{21}(t) + 2C_{22}(t)$ is equivalent to $\langle D^2_{00}(\delta\Omega(t))\rangle$, where $\delta\Omega(t)$ is the variation of the set of Euler angles due to molecular rotation. Expression (1) has been taken in such a complicated form, which is normally used for two-variable correlation functions [13] to eliminate systematic errors due to the long time fluctuations of the orientational ordering to which the slowly decaying correlation functions are very sensitive. When we study the re-orientation of bonds, the reason for taking only the $D^L_{m0}(\Omega(t))$ functions with the first lower index positive and the second index equal to zero is obvious: we account for the axial symmetry of a vector connecting any two atoms and the axial symmetry of the

simulated ensemble. For the whole molecule this set is certainly not complete. If the intrinsic molecular coordinate system is identified with that of the molecular moment of inertia tensor, it becomes obvious that flexible PCH5 molecules are far from uniaxial symmetry, and hence the second index has to range from $-L$ to L. In general, the rank L of the two D functions constituting the time autocorrelation function can also be different (see Chapter 6 of [2]), but normally only those with equal rank contribute to experimentally observable properties. So, to save space, we shall not present here the less relevant autocorrelation functions; they are available from the authors on request.

3.2. *Dynamics of the simulated molecules*

Orientational autocorrelation functions for different molecular bond vectors have been derived for both phases from the simulation data, as shown in figure 1. The infinite time value for all of these functions in the nematic phase is zero and does not depend on the static orientational ordering of the various fragments. Nevertheless, the orientational relaxation rate differs for different vectors, even those which are more or less parallel to the long molecular axis, indicating molecular flexibility. Differences are even observed within the rigid molecular core. The relaxation rates increase for the more flexible fragments (a dynamic even–odd effect can be noted in the alkyl chain). A similar feature is observed also for the short-time decay. The fact that molecular flexibility contributes to the short-time decay of the orientational CFs of molecular fragments is confirmed by figure 2 where their reorientational movement is compared with that of the whole molecule.

The molecular flexibility can effect the reorientational CFs of the bonds in two ways:

(i) Intermolecular forces which reorient the whole molecule relatively slowly can lead to fast movements of molecular fragments and hence to the fast initial decay of the corresponding CFs. The weaker the connection of the fragment with the rigid core the stronger this initial decay (figure 1), its time-scale being consistent with the time scale of the torques acting on the molecule (figure 3). The long time decay of the CFs is quite similar for different molecule fixed vectors and is caused by the reorientation of the molecule as a whole.

(ii) In different molecular conformations the bond can be substantially declined from the molecular principal axis and rotation around other axes can contribute to the relaxation of the corresponding CF. Even for the cyano bond this means that not only tumbling but also the faster spinning motion can contribute to the short-time, fast decay.

One way of checking this hypothesis would be to simulate a system of rigid molecules in an all-*trans* conformation. The dynamical and most of all the static properties of such a system will be very different. This can substantially change the dynamical processes and mislead the comparison. Therefore we simulated a system of rigid molecules by starting from one of the configurations of the isotropic ensemble. The actual molecular conformations were frozen in by increasing the intramolecular potential barriers to such an extent that any conformational changes were suppressed during the whole simulation run. As a result, the static parameters (like order parameters) were not changed (see table 1). From figure 4 it is seen that the time of the reorientation of the molecule as a whole (the long-time slope of the

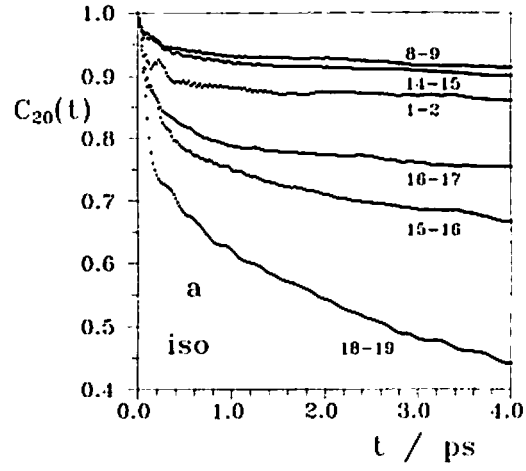

(*a*)

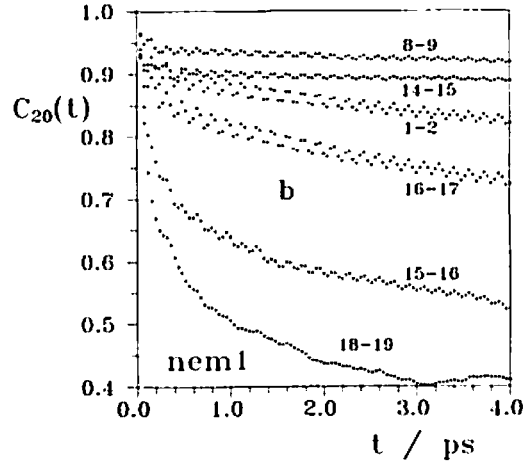

(*b*)

Figure 1. Orientational autocorrelation functions for different bonds (marked by the numbers of the atoms shown in 1) of the PCH5 molecule in the (*a*) isotropic and (*b*) nematic phases.

1–19 CF) was not changed. Nevertheless, some changes of the librational movement are clearly seen.

Comparing the behaviour of the CFs of the cyano bond for these two cases (see figure 4) one can conclude that the influence of the intramolecular flexibility under persistent intermolecular forces is substantial, but that it is not the only one contributing to the CFs decay. The difference between the cyano bond CFs in rigid and non-rigid molecules is especially striking, bearing in mind the almost identical behaviour of the torque CFs for these systems (figure 3(*a*, *c*)). Both the aforementioned mechanisms affect the CFs for non-rigid molecules. The importance of the spinning motion contribution is indicated by the fact that the rate of the short-time decay (up to 0·5 ps) is almost identical for the cyano bond, and for the 3–4 C–C bond within

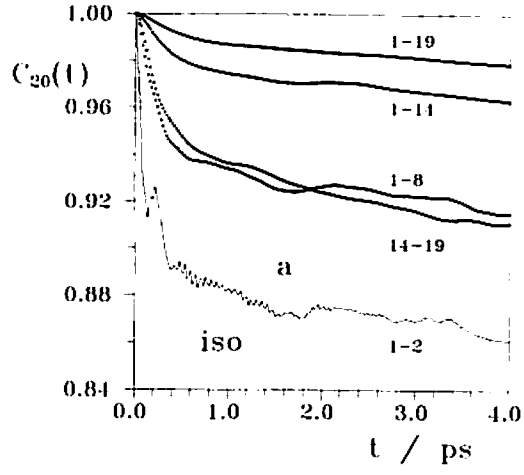

(*a*)

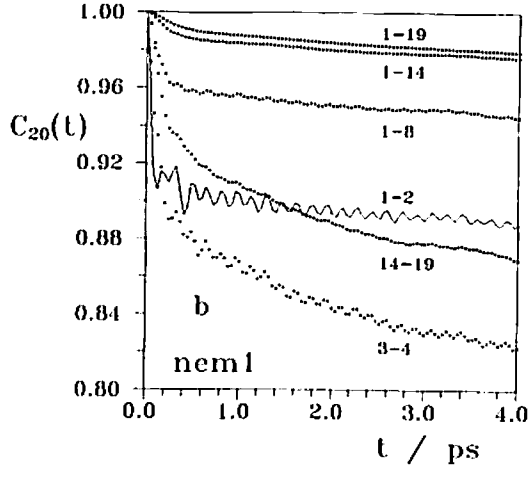

(b)

Figure 2. Orientational autocorrelation functions for different fragments (marked by the numbers of the lateral atoms; 1–19, for example, corresponds to the whole molecule) in the (*a*) isotropic and (*b*) nematic phases.

the benzene ring, whose relaxation is definitely strongly affected by the molecular spinning motion (figures 2(*b*) and 4). That is true for both kinds of system.

It is difficult to describe precisely the contribution of the spinning motion. One can consider the spinning motion of the whole molecule with the help of D functions with $m = 0$ and a non-zero second lower index. But this refers to a coordinate system

Figure 3. Autocorrelation functions of the absolute value of the torque acting on the PCH5 molecule in the (*a*, *c*) isotropic and (*b*) nematic phases and its projections in cyclic basis sets [25], of different symmetry. The Γ_{Lm} are defined in a similar way to C_{Lm} by formula (1) except that Ω in this case means the orientation of the torque. Γ_{10} corresponds to the z projection while the other one can be related to the x and y components in the Cartesian frame.

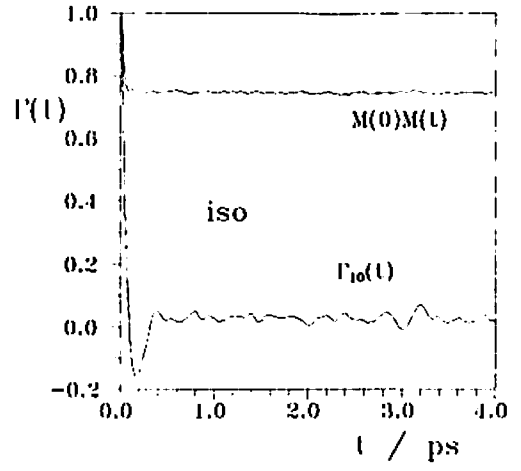
1.0
0.8
0.6
0.4
0.2
0.0
−0.2
Γ(t)
M(0)M(t)
iso
Γ10(t)
0.0
1.0
2.0
3.0
4.0
t / ps

(*a*)

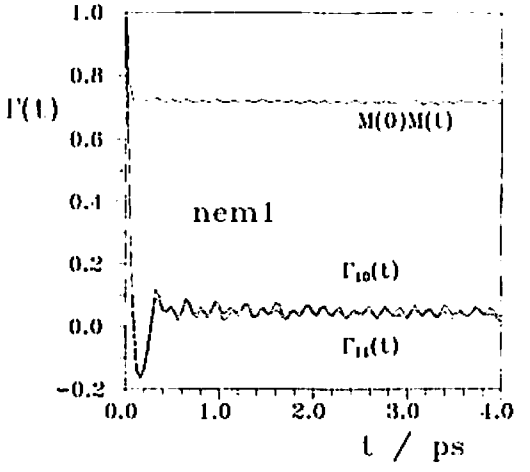
1.0
0.8
0.6
0.4
0.2
0.0
−0.2
Γ(t)
M(0)M(t)
nem1
Γ10(t)
Γ11(t)
0.0
1.0
2.0
3.0
4.0
t / ps

(*b*)

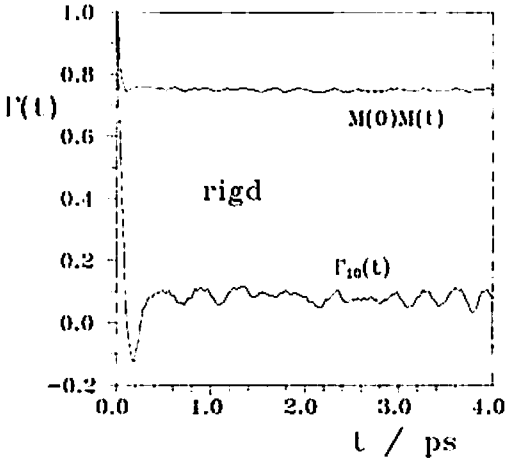
1.0
0.8
0.6
0.4
0.2
0.0
−0.2
Γ(t)
M(0)M(t)
rigd
Γ10(t)
0.0
1.0
2.0
3.0
4.0
t / ps

(*c*)

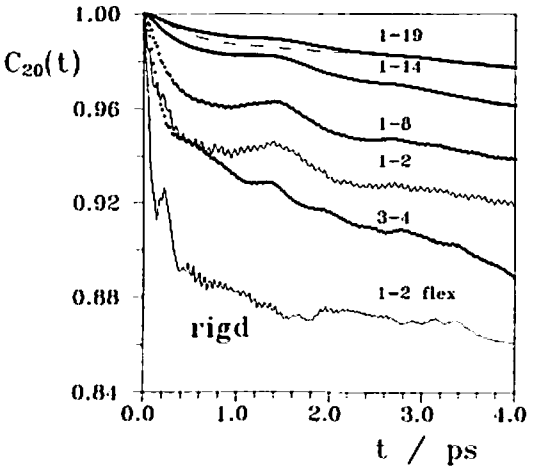

Figure 4. Orientational autocorrelation functions for different fragments of rigid PCH5 molecules in the isotropic phase. The CF for the cyano bond (1–2 in figure 2(*a*)) of the flexible molecules is also presented for comparison. The CF of the whole flexible molecule (1–19 in figure 2(*a*)) is plotted as the dashed line.

which is fixed to the principal axes of the moment of inertia tensor, and therefore will be subject to fluctuations in the molecular conformation. Hence both kinds of motion are strongly coupled.

To treat the effect of intramolecular motions and molecular flexibility in more detail, we calculated also orientational autocorrelation functions for different fragments in an internal molecular frame (the frame of the benzene ring has been taken for this as the most slowly reorienting in the external frame). Two regions are well distinguished also in all internal CFs (for example for bond 16–17 in figure 5). The long-time decay resembles diffusional motion with correlation times of the order of hundreds of picoseconds, but the short-time decay looks more like that of librational motion. When calculating the internal correlation functions, we assumed cylindrical symmetry of the molecule, and hence the $C_{Lm}(t)$ with $m \neq 0$ corresponding to twisting motions around the long axis of the fragment. It is evident from figure 5, that this twisting motion (and probably also torsional motions within the molecular tail) strongly randomize the molecular conformation within half a picosecond. This certainly does not mean the absolute randomization of the orientation of the relevant molecular fragment (see, for example, the CF in the external frame represented by the solid line in figure 5). This process probably governs the short-time behaviour of the orientational CFs in the external frame.

Comparing the order parameters for different bonds in the molecular frame (table 2), one can conclude that the changes of the N–C–C angle contribute negligibly to the declination of the cyano bond from the molecular long axis; the order parameter of the cyano bond in this system is very high. Nevertheless, the movement of the fragments placed in the opposite ends of the molecule or rather their conformations are correlated. From table 3 it is seen that the value of the normalized cross-correlation factor (the Ω_i refer to the benzene ring fixed frame)

$$g_{Lm} = \frac{\langle [D^L_{m0}(\Omega_1) - \langle D^L_{m0}(\Omega_1)\rangle][D^{L*}_{m0}(\Omega_2) - \langle D^{L*}_{m0}(\Omega_2)\rangle]\rangle}{[\langle |D^L_{m0}[\Omega_1]|^2 - |\langle D^L_{m0}[\Omega_1]\rangle|^2\rangle\langle |D^L_{m0}[\Omega_2]|^2 - |\langle D^L_{m0}[\Omega_2]\rangle|^2\rangle]^{1/2}}, \quad (2)$$

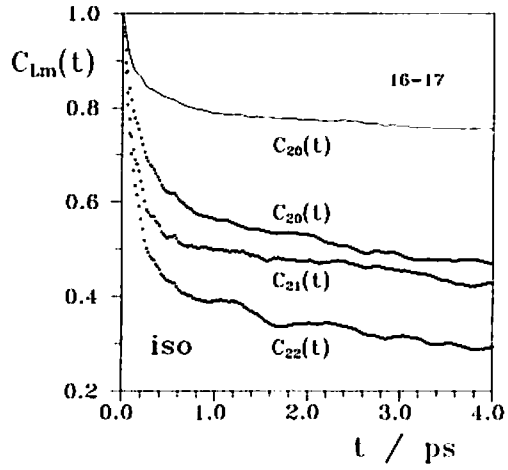

Figure 5. Orientational autocorrelation functions of different symmetry for the 16–17 bond in the molecular fixed frame (dots) and in the external frame (solid curve). The data were obtained for the isotropic ensemble.

characterizing the correlations between the deviations of different bonds from their average orientation in the internal molecular frame, is sufficiently high.

To study quantitative differences in the short-time behaviour of the various fragments it is convenient to expand the corresponding CFs defined by equation (1) into a Taylor set around zero:

$$C_{Lm}(t) = 1 - \ddot{C}_{Lm}(0)t^2/2! + \ddot{\ddot{C}}_{Lm}(0)t^4/4! + \cdots \tag{3}$$

For isotropic liquids constituted of cylindrically symmetric molecules the second derivative (the normalized second spectral density moment) is [17]

$$\ddot{C}_{Lm}(0) \equiv \ddot{C}_{L0}(0) = \frac{L(L+1)kT}{I}, \tag{4}$$

where I is the moment of inertia for the short molecular axis, k is the Boltzmann constant, and T is the temperature. By fitting the first two terms of this expansion to the experimental curves, it is possible to estimate effective moments of inertia of the rotating units. For an anisotropic phase the $\ddot{C}_{Lm}(0)$ depend on the order parameters [14]. Using the results of [14] one can derive the formulae for the

Table 2. Order parameters $\langle P_2 \rangle$ for various molecular fragments in the benzene ring fixed molecular frame for the nematic and isotropic phases.

	Bond			
System	1–2	14–15	16–17	18–19
Iso	0·926	0·768	0·591	0·413
Nem1	0·923	0·817	0·645	0·564

Table 3. Factors g_{Lm} for the correlation between 1–2 and other bonds within the PCH5 molecule obtained with formula (2) for the nematic phase, nem1.

Bond	8–9	14–15	16–17	18–19
g_{10}	0·154	0·091	0·151	0·167
g_{11}	0·210	0·168	0·086	0·054

Table 4. Second derivatives $\ddot{C}_{Lm}(0)$ of the orientational CFs of the moments of inertia tensor for different simulated systems estimated directly from the CF2 (Sim) and from equations (4) and (5) (Comp), using the molecular moments of inertia ('Comp, fragment 1–19' in table 5). The values are represented in ps^{-2}. The uncertainty of all the simulation results is about 20% and that for the computed ones is 5%. P_4 was taken as 0·315 and 0·29 for nem1 and nem2, respectively.

	Iso		Rigd		Nem1		Nem2	
	Sim	Comp	Sim	Comp	Sim	Comp	Sim	Comp
$\ddot{C}_{20}(0)$	0·30	0·36	0·26	0·37	0·48	0·71	0·50	0·71
$\ddot{C}_{21}(0)$					0·52	0·64	0·54	0·64
$\ddot{C}_{22}(0)$					0·68	0·94	0·70	0·94

normalized CFs defined by equation (1) and obtain from equation (3):

$$\left.\begin{aligned}
\ddot{C}_{20}(0) &= \frac{42 + 30\langle P_2\rangle - 72\langle P_4\rangle}{7 + 10\langle P_2\rangle + 18\langle P_4\rangle - 35\langle P_2^2\rangle}\,\frac{kT}{I} \\
\ddot{C}_{21}(0) &= \frac{42 + 15\langle P_2\rangle + 48\langle P_4\rangle}{7 + 5\langle P_2\rangle - 12\langle P_4\rangle}\,\frac{kT}{I} \\
\ddot{C}_{22}(0) &= \frac{42 - 30\langle P_2\rangle - 12\langle P_4\rangle}{7 - 10\langle P_2\rangle + 3\langle P_4\rangle}\,\frac{kT}{I}.
\end{aligned}\right\} \tag{5}$$

Fits to the simulated CFs have been done between zero and 0·05 ps, and the resulting second derivatives are summarized in table 4. The values of the moments of inertia estimated with equations (4) and (5) for different phases and different systems are presented in table 5. As is clear from definition (1), this corresponds to an average of two maximal eigenvalues of the moment of inertia tensor. Such values, estimated directly from molecular configurations are also presented in table 5.

It should be noted that for all of the systems studied the second derivative of the autocorrelation functions of the whole molecule are systematically smaller than estimated from the relevant moments of inertia. This indicates the strong effect of the molecular interactions (which were neglected in the estimates) in agreement with the very short correlation time for the molecular torque which is observed in figure 3. Even within this very short time interval of 0·05 ps it is not possible to observe totally free rotation. The effect of the molecular interaction depends strongly on the kind of CF, being maximal for $\ddot{C}_{20}(0)$. Therefore the averaged $\ddot{C}_{Lm}(0)$ values were taken for the moments of inertia estimates in table 5 (sim). Comparison of the data in different rows of table 5 gives a quantitative illustration of the effect of

Table 5. Moments of inertia of various molecular fragments calculated directly from molecular configurations (Comp); averaged values obtained from $\ddot{C}_{Lm}(0)$ with equations (4) and (5) (Sim); from Raman investigations of the cyano stretching mode [7] (Exp). The I values are in 10^{-46} kg m^2.

	Iso		Rigd		Nem1		Nem2	
Fragment	Sim	Comp	Sim	Comp	Sim	Comp	Sim	Comp
1–19	1010	842	1160	814	1060	849	1030	848
1–8	49	58	43	60	59	61	62	61
1–2	11	1·9	11	1·9	11	1·9	9·8	1·9
1–2 Exp		13±2				27±9		

flexibility and/or spinning motion on the short-time decay of molecular fragment reorientation.

Concluding the treatment of the short-time reorientational motion of the simulated flexible molecules, one can deduce the following picture: on the one hand, being subjected to strongly fluctuating intermolecular forces, the conformation of the molecules exhibits relaxation in a time scale which is much shorter than that expected from the corresponding molecular moments of inertia; on the other hand, this conformational flexibility couples the contributions of molecular rotations around different axes to the orientational relaxation of a molecular fragment.

3.3. *Comparison with experiment*

From a band shape analysis of Raman spectra the orientational autocorrelation function for the cyano bond of isotropic PCH5 has been derived (see figure 6), and this can be compared with the simulated ones. The initial non-exponential decay is observed well in the experimental and the simulated curves for different fragments in both phases (see also figure 1).

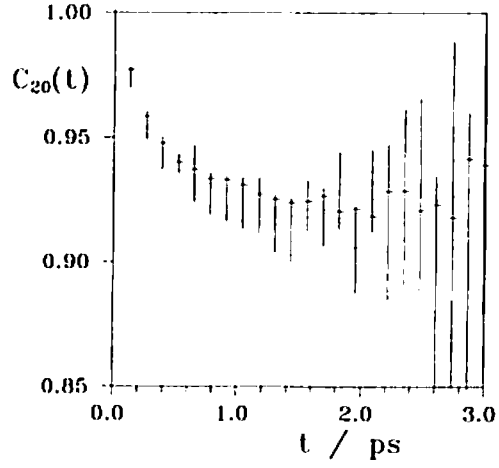

Figure 6. Experimental CF for the cyano fragment reorientation, obtained from Raman band-shape analysis in the isotropic phase at 333 K.

Evidence that only the rotation of some molecular fragment is observed in Raman experiments can be obtained from a comparison of the moments of inertia derived from experimental autocorrelation functions, by using equations (4) and (5), with average values calculated for the short molecular axes from the simulated configurations (table 5). Certainly the experimental values are influenced by the molecular interactions, but this can only increase the apparent values. In spite of this, experimental values are comparable only with the moments of inertia of small molecular fragments.

Thus, experimental data have shown that the short-time non-exponential relaxation is not an artefact of the simulation procedure, but represents a phenomenon which has to be taken into account in appropriate models.

3.4. *Memory functions formalism*

Criteria for choosing an appropriate model to describe the rotation of mesomorphic molecules can be derived from a formal analysis based on the memory-functions approach [15]. So we must choose which angular variable we can treat as Markovian, i.e., the frequency dependence of which can be neglected. The short-time evolution of the orientational CFs, which is most interesting here, occurs within the time scale of the molecular interaction relaxation (comparison of figures 3 and 1), preventing a time-scale separation at this level. Thus we can conclude that in order to be able to describe the features of interest, the model should not neglect the time evolution of the torque from intermolecular forces. Consequently, we can be sure that small-step [16] or extended [17] diffusion models cannot provide a comprehensive description. Proper theories, like cage models [18], must treat angular momentum and torque as dynamical quantities, and only the derivative of the torque (or higher order derivatives) can be treated as Markovian. Nevertheless, at first we shall distract our attention from the particular shape of the CFs, and analyse only the long-time diffusive behaviour; the more appropriate cage models will be treated after this.

3.5. *The diffusion model*

Most of the work on the re-orientational dynamics of molecules in liquid crystals is devoted to the long-time behaviour. Orientational relaxation is treated as a diffusion in an external potential, usually of mean-field type, while the results do not depend on the particular form of the mean-field potential. Thus, in [19] and [20] orientational correlation times for D functions of different symmetry were derived, using the small-step diffusion model for molecular orientational relaxation in the mean-field nematic orienting potential:

$$\left.\begin{aligned}
\tau_{20} &= \frac{7 + 10\langle P_2\rangle + 18\langle P_4\rangle - 35\langle P_2\rangle^2}{6D_r(7 + 5\langle P_2\rangle - 12\langle P_4\rangle)},\\
\tau_{21} &= \frac{7 + 5\langle P_2\rangle - 12\langle P_4\rangle}{6D_r(7 + 2{\cdot}5\langle P_2\rangle + 8\langle P_4\rangle)},\\
\tau_{22} &= \frac{7 - 10\langle P_2\rangle + 3\langle P_4\rangle}{6D_r(7 - 5\langle P_2\rangle - 2\langle P_4\rangle)},
\end{aligned}\right\} \qquad (6)$$

Table 6. Orientational correlation times for two nematic systems (with different partial charges) from an exponential fit $C(t) = A\exp(-t/\tau)$ to the long-time tail of the simulated CFs (fragment 1–19). Results from a small-step diffusion theory [20] are also given. The values in parentheses are the corresponding As. The accuracy was estimated to be 10% for the τ values and 2% for the A values.

Parameter	Nem1 (Cyano)	Nem1 (Whole)	Theory Eq. (6)	Nem2	Theory Eq. (6)
τ_{20}(ps)	1750 (0·85)	1900 (0·974)	2400	620 (0·970)	760
τ_{21} (ps)	950 (0·76)	2100 (0·972)	1600	800 (0·976)	490
τ_{22} (ps)	1050 (0·765)	1500 (0·961)	1500	570 (0·960)	460
τ_{20}/τ_{21}	1·84	0·90	1·54	0·78	1·54
τ_{20}/τ_{22}	1·67	1·27	1·64	1·09	1·64
τ_{21}/τ_{22}	0·90	1·40	1·07	1·40	1·07

where D_r is the diffusion coefficient for molecular tumbling, which has been derived from the simulations in [10]. The results of the calculation for the relaxation times and their ratios are presented in table 6.

As it is seen from figure 2, in the long-time limit the correlation functions of both the whole molecule and its fragments can be well approximated by a single exponential. This is illustrated by the multi-exponential least-squares fit of one of the simulated CFs for Nem1 in the time interval 0–100 ps:

$$C_{20}(t) = 0{\cdot}9735\,e^{-t/1900} + 0{\cdot}014\,e^{-t/14} + 0{\cdot}0125\,e^{-t/0{\cdot}5}. \qquad (7)$$

For the system with smaller partial charges the short-time exponents have even smaller relaxation times.

We have performed single-exponential fits for two nematics with different partial charges in the time interval 10–100 ps (the lower limit was taken relatively high to ensure the applicability of the one-exponent approximation). The orientational relaxation times were strongly dependent on the partial charges: the bigger the charges the longer the duration of the relaxation. But the ratios are not so different for the simulated ensembles (although the difference is somewhat larger than the computational uncertainty).

Comparing the simulated data with the theoretical predictions one can conclude that the absolute values of the relaxation times are well predicted by the Kirov *et al.* [20] expressions, but they fail to predict correct ratios of the correlation times. One of the severe approximations used in [20] is the one-exponent approximation. But as it is shown in [21] (see also Chapter 3 in [2]) this does not lead to substantial changes. Probably, the residual differences can be attributed to the effect of molecular flexibility, which can strongly affect $C_{21}(t)$ and $C_{22}(t)$.

3.6. *Cage parameters*

Before testing the cage models it is useful to investigate the parameters of the cage, and the extent to which the interactions of a molecule with its surroundings can be described by the cage effect. Simulated configurations can be used as a source of direct information on the cage dynamics, like in the recent work by Moro *et al.* [22] on Lennard–Jones liquids. So, for a given configuration we considered the interaction energy of a chosen molecule i with the rest of the simulation box (with

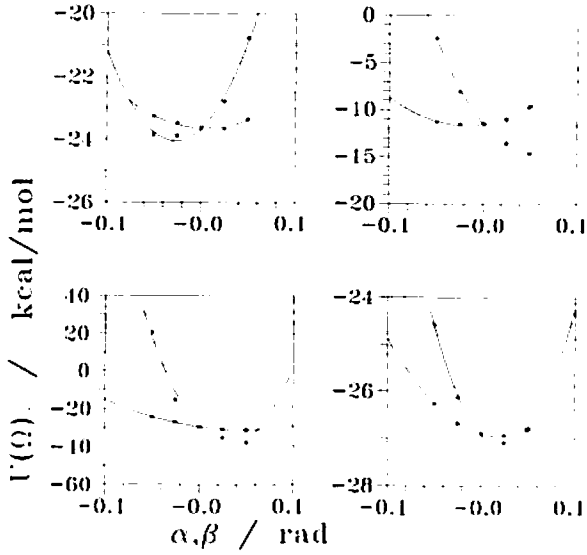

Figure 7. Examples of the dependence of the cage potential on the orientation for some arbitrarily chosen molecules of simulated PCH5 in the isotropic phase (asterisks). The curves are the least-squares parabolic fits of the computed results. The dashed curves correspond to the re-orientation in the plane of the benzene ring, and the solid curves to re-orientations perpendicular to it.

cut-off limits similar to those used during the simulation run)

$$U_i(R_1, \Omega_1, \ldots, R_i, \Omega_i, \ldots, R_N, \Omega_N) = \sum_{j \neq i} u(R_i, \Omega_i, R_j, \Omega_j). \tag{8}$$

By changing the orientation of the reference molecule i (the rest being fixed) we obtain a potential surface for the molecule under consideration:

$$U_i(\Omega) \equiv U_i(R_1, \Omega_1, \ldots, R_i, \Omega, \ldots, R_N, \Omega_N). \tag{9}$$

Examples of such potentials for some molecules in the isotropic phase of the system considered can be seen in figure 7. Only small deviations from the actual molecular positions have been considered because of the steepness of the potential in most cases, confirming the idea of the cage. In an internal molecular frame we distinguished between the reorientations in different planes: in the plane of the benzene ring (yz plane, or angle β in figure 7) and perpendicular to it (xz plane, or angle α in figure 7). The variations in the well shape and its deviations from the harmonic potential can be observed in this figure. Nevertheless, as was noted in [22], one can approximate the well by a harmonic function (due to the small deviations of the instant orientations from their minimum position for most molecules):

$$U(\beta) = K\beta^2/2, \tag{10}$$

attributing anharmonic terms to fast fluctuating intermolecular forces. Here, β can be any of the angles describing the molecular orientation in the well, either in the intrinsic molecular system or in the coordinate system of the director (see figure 8). The fluctuations in the curvature could be treated similarly if the fluctuations are not too high. To test this, the potentials were approximated by a parabola in the

Table 7. Parameters of the molecular motion within the cage and the cage parameters for the isotropic and nematic phases of PCH5; for explanations see the text (kcal = 4·1868 kJ).

	Iso	Nem1
Average potential curvature K (kcal mol^{-1} rad^{-2})	857	590
Curvature relaxation time (ps)	0·15	0·06
Mean-square displacement of the molecules within the cage (mrad)	74	66
Average libration period estimate (ps)	0·48	0·64

vicinity of the bottom, yielding distribution functions for the curvature in different planes. As can be seen from figure 8 for both planes of re-orientation the distribution functions are almost identical and very broad. The high probability of very low curvature indicates that presumably due to the complicated shape of mesogen molecules their packing is far from being dense. Moreover, the width of the distribution shows that the fluctuations cannot be treated as being small. It seems that larger reorientation jumps of the mesogen molecules proceed during fluctuations of the barrier between adjacent wells to low values (a very small amount of states with negative curvature corresponds to molecules which are near the saddle point). The summary of the main properties of the cage potential both for nematic and isotropic states is presented in table 7.

After determining the position of the minimum of the well in the aforementioned coordinate systems, the position of each molecule relative to this minimum has been determined. Looking at the instant positions of the molecules in the well (figure 9(*c*)) it is difficult to see any anisotropy in the projection to the *xy* plane. For the nematic phase even the distribution functions describing the orientation in the *xz* and *yz* planes displayed in figure 9(*b*) are similar, so we neglected any deviations.

In the nematic phase it is natural to study the cage parameters in the coordinate system fixed to the director frame. The β and α in the distributions of figures 8(*b*) and 9(*b*) correspond to polar (α = const and β variable), and azimuthal (β = const and α variable) angles. The similarity between the cage curvature (figure 8(*b*)) and cage orientation (figure 9(*b*)) distributions in different planes in the nematic phase can be used as a simplifying factor in cage theories of the mesophase. It should be noted that an increase of the orientational ordering in the mesophase results in a better defined cage shape: the orientational distribution function of the molecules within the cage becomes narrower and the mean-square deviation of the molecular orientation in the cage is smaller (table 7). This increase in the order leads to a decrease in the average cage curvature (table 7) due to the substantially smaller amounts of molecules placed very far from the bottom of the well, where the interactions are much higher than predicted by a simple parabola. Nevertheless, even in the nematic phase the cage is far from ideal: the fraction of cages with a curvature close to zero is very large. The origin of these contributions can be seen from figure 8(*c*), where the mean cage curvature is displayed as a function of the position of the potential minimum relative to the director. The cages directed perpendicular to the director ($P_2 = -0{\cdot}5$) have the smallest curvature. Such a strong dependence is not obvious, and commonly (see, e.g., [23]) the short range (isotropic) potential is supposed to have a much higher curvature than the mean field one. From these

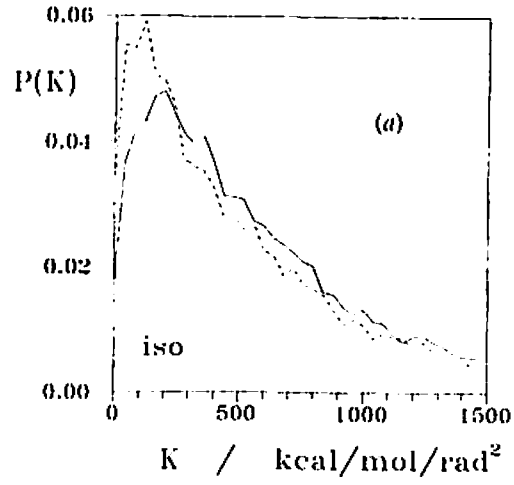
0.06
P(K)
0.04
0.02
0.00
(a)
iso
0
500
1000
1500
K / kcal/mol/rad²

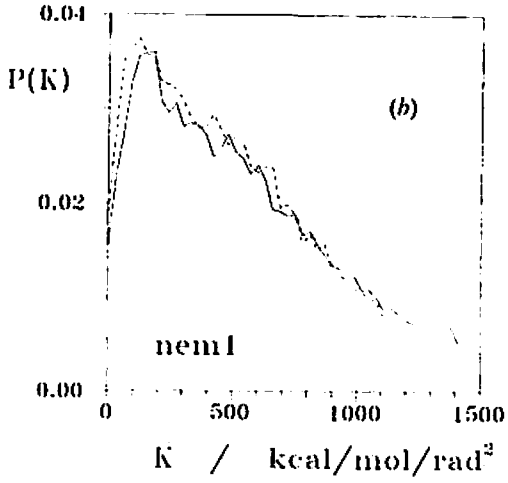
0.04
P(K)
0.02
0.00
(b)
nem1
0
500
1000
1500
K / kcal/mol/rad²

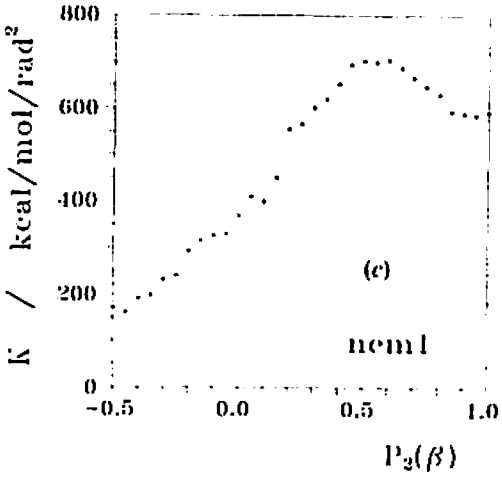
800
600
400
200
0
K / kcal/mol/rad²
(c)
nem1
-0.5
0.0
0.5
1.0
P₂(β)

studies we can conclude that the macroscopic anisotropy of the mesophase manifests itself in modifying the parameters of the short range potential.

To study the dynamical properties of the cage and the molecule in it we separated the re-orientational movement of the cage from changes in its shape. The visualization of the time evolution of a particular molecule's orientation and its cage (figure 10) suggests that while the molecular orientation is evolving in a continuous way the cage motion, being dependent on the spatial variables of a large number of molecules, is much more erratic. Under these circumstances pronounced molecular librational motions within the well cannot be observed. In fact an average molecular libration period

$$T = \frac{1}{2\pi}\left(\frac{I}{K}\right)^{1/2}, \tag{11}$$

as calculated with average values for I and K taken from tables 5 and 7, would last much longer than the time necessary for a change in the curvature of the cage (compare figure 11 and table 7). This does not mean that the cage disappears; its curvature becomes non-zero, but completely non-correlated with its initial value. Due to this dynamic averaging we can summarize that at least in the isotropic case the molecules are placed in similar rapidly fluctuating cages. Unfortunately, due to very fast changes in the shape of the cage we cannot distinguish whether the re-orientation of the molecule occurs due to the transition to another cage, or whether the same cage is reorienting.

3.7. *The cage model*

Some cage models of the rotational motion of non-spherically symmetric molecules have been developed for isotropic liquids [18, 24]. According to them the molecule has several stable orientations, i.e., potential minima of the orientational energy. The height of the barriers separating the minima must be larger than kT to ensure the oscillatory movement of the molecule. The molecule is subject to a random force from the surroundings and hence its libration is damped. When the energy fluctuations reach the height of the potential barrier, the molecule leaks out of the well into a neighbouring one. For a two-dimensional potential of this kind the equations for rotational motion have been solved [18], resulting in the orientational autocorrelation function

$$\begin{aligned}\rho_{mn}(t) &= \langle \exp\left[in\theta(0) - im\theta(t)\right]\rangle \\ &= \exp\left(-2\gamma t\right)\delta_{mn}\left(\exp\left[-\frac{kTn^2}{K}\left\{1 - u_{11}(t)\right\}\right] - \exp\left[-\frac{kTn^2}{K}\right]\right. \\ &\qquad \left.\times\left\{1 - \exp\left[2\gamma t\cos\frac{2\pi n}{N}\right]\right\}\right).\end{aligned} \tag{12}$$

Figure 8. Distribution functions of the cage curvatures defined by equation (19) in different planes for the (*a*) isotropic and (*b*) nematic phases. In part (*a*) the dashed line corresponds to the re-orientation in the plane of the benzene ring, and the solid line to re-orientation perpendicular to it. In part (*b*) the solid and dashed lines correspond to polar β and azimuthal α angles, respectively, in the director fixed frame. In part (*c*) the mean cage curvature is displayed as a function of the position of the potential minimum relative to the director.

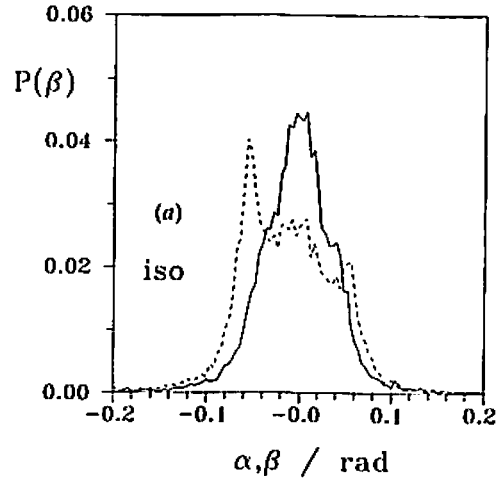
0.06
P(β)
0.04
(a)
iso
0.02
0.00
−0.2
−0.1
−0.0
0.1
0.2
α,β / rad

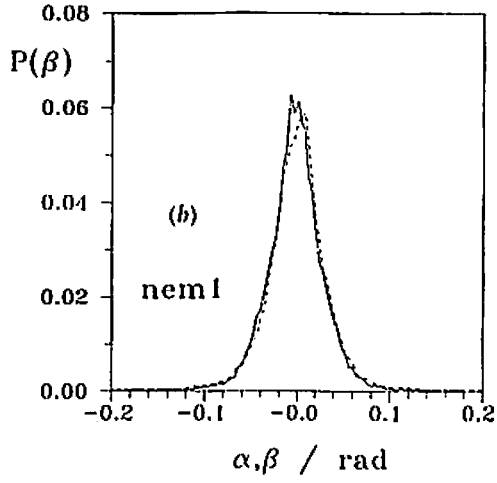
0.08
P(β)
0.06
0.04
(b)
nem1
0.02
0.00
−0.2
−0.1
−0.0
0.1
0.2
α,β / rad

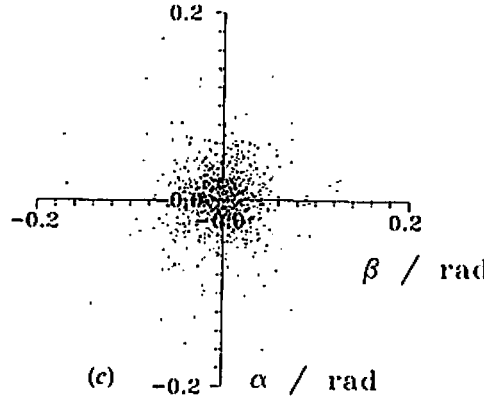
0.2
−0.2
0.2
β / rad
(c)
−0.2
α / rad

where

$$u_{11}(t) = \exp\left(-\frac{\eta t}{2}\right)\left[\cos \Omega t + \frac{\eta}{2\Omega} \sin \Omega t\right] \tag{13}$$

and

$$\Omega = \left(\frac{K}{I} - \frac{1}{4}\eta^2\right)^{1/2}. \tag{14}$$

K is the force coefficient as defined by equation (10); N is the number of wells within 2π. The rate γ of escaping the well can be related to these parameters and to the damping factor η. It is worth noting that $\rho_{22}(t)$, for example, is a linear function of $C_{20}(t)$, defined by equation (1). (Explicit expressions for the Wigner D functions can be found in [25].)

In the itinerant oscillator model [26] a non-spherical molecule librates inside a cage of neighbouring molecules. The cage in its turn performs rotational Brownian motion. Analytical solutions for discs in two dimensions have the form of equation (12) which we shall discuss.

This equation combines resonance and diffusional phenomena as can be seen by putting $t \ll \gamma$, or $t \gg \eta$. Extrapolation of its long-time part to $t = 0$ intersects the y axis at $\ln(\rho_{nn}(t)) = -(kTn^2/K)$ below zero, similar to experimental and simulated curves. From the previous considerations most of the model parameters (I, K) are already defined. The number of wells can be taken rather arbitrarily: this is strongly coupled in the model to γ and determines only the long-time relaxation. From the width of the distribution function in figure 9 one might accept 16 to be a reasonable estimate. This value ensures also sufficient deepness of the wells. γ has been derived from the long-time slope of the autocorrelational functions. The value of the last arbitrary parameter η was varied to minimize the oscillatory behaviour. The resulting model autocorrelation curve is compared to the experimental one in figure 12(*a*), curve 1; the list of the parameters values is summarized in table 8.

It is seen that the average value of the cage potential curvature derived from the simulations is not able to describe the initial decay of the orientational relaxation (this decay is totally determined by kTn^2/K in equation (12)). Inertial effects cannot make the initial decay more substantial; a smaller η only increases the amplitude of librations and smaller moments of inertia I make the short-time relaxation faster, but not deeper. Here, we see again a manifestation of the non-uniformity of the cage potential curvature, i.e., the contribution of the cages with nearly zero curvature. As can be seen from figure 12(*a*), only with much smaller value of K (curve 2, and table 8) it is possible to achieve the required magnitude of the short-time decay. For a correct description of the time evolution of the reorientational CFs in the whole time interval, one has to account for the distribution of the cage curvatures.

From figure 12(*b*) it is seen that the cage model can predict, in principle, the evolution of the CFs for molecular fragments. The curvature K in this case can be chosen arbitrarily and can lose any physical meaning, while the moments of inertia can be taken as estimated from the atomic spatial structure of the separate molecular fragments (compare tables 5 and 8).

Figure 9. Distribution functions of the molecular orientation in the cage for (*a*) isotropic and (*b*) nematic phases in different planes. Part (*c*) is a scatter plot illustrating the instant orientations of molecules in the cage. The correspondence of the different curves is similar to that in figure 8.

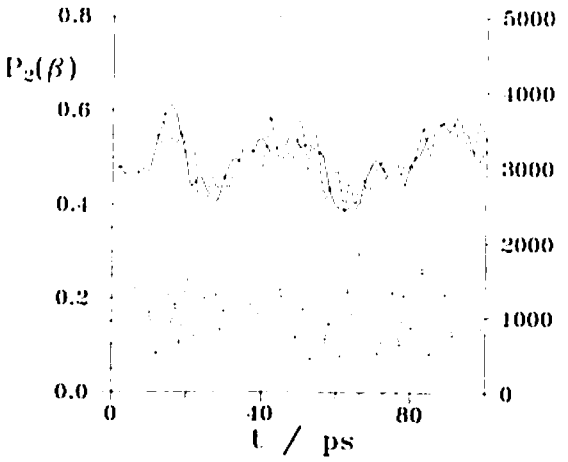

Figure 10. Time dependence of the orientation of a particular molecule (solid line) and the orientation of its potential well (dashed line) in the nematic phase. The orientation is described by the azimuthal angle in the director frame. The lower curve is the plot of its potential curvature time dependence. The time step of the plot is 0·2 ps.

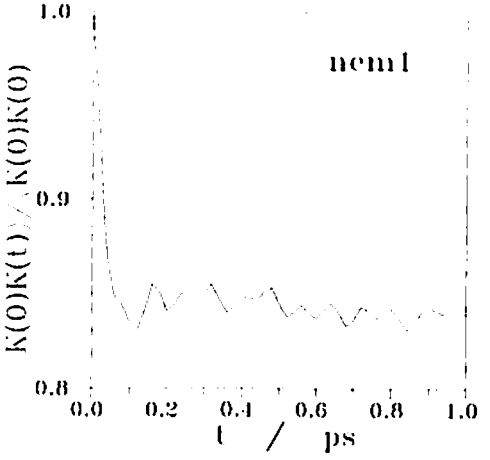

Figure 11. Autocorrelation function of the curvature of the cage for the nematic phase PCH5.

Table 8. Model parameters used in equations (12–14) to fit the simulated CFs in figure 12. For an explanation of the parameter values see the text.

	γ/ns^{-1}	$I/10^{-46}$ kg m^2	$(kT/K)/10^{-3}$	η/ps^{-1}
Curve 1	0·5	842	0·767	16
Curve 2	0·5	842	4·83	6
Curve 3	2·63	1·9	30·4	56

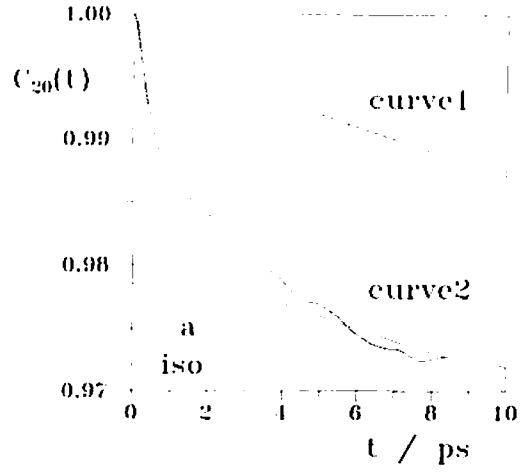

(*a*)

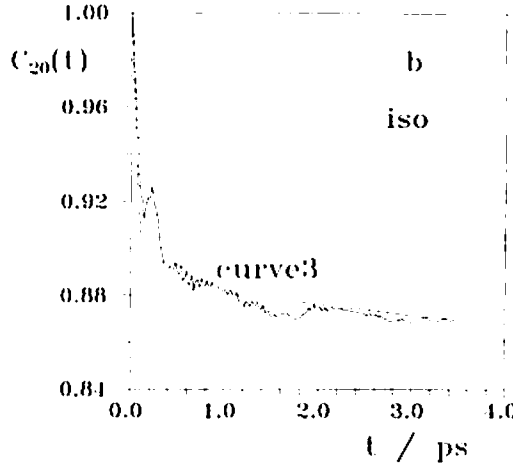

(b)

Figure 12. The re-orientational autocorrelation functions of (*a*) the whole molecule and (*b*) the cyano bond in the isotropic phase, obtained from simulations (solid curves) and from the cage model (dashed curves) with equations (12–14). The fitted parameters are given in table 8.

4. Conclusion

In this computer simulation study of tumbling molecular motion in mesomorphic systems we used the typical mesogen PCH5, bearing in mind the possibility of extending our conclusions to other nematic compounds. It became evident that the conformational molecular flexibility plays an important role, not only in the orientational statistics of the molecules in the mesophase, but also in their dynamics. We analysed orientational autocorrelation functions of different molecular fragments in both frames of the nematic director and in an internal molecular frame within the time interval 1–100 ps. From these studies we can conclude that molecular orientational

motion can be described well by the diffusion model only at sufficiently long time intervals (not less than 1 ps). To observe single exponential orientational diffusion even larger time intervals (more than 10 ps) must be treated. The short-time orientational movement is driven by other mechanisms: on the one hand, being subjected to strongly fluctuating intermolecular forces, the conformation of the molecules exhibits relaxation in the same time-scale, which is much shorter than that estimated from corresponding molecular moments of inertia. This results in a very fast short-time relaxation of the re-orientational CFs. On the other hand, this conformational flexibility couples molecular rotations around different axes, causing the spinning and twisting molecular motions to contribute to the tumbling molecular motion. This can be probed by studying the properties of single fragments.

In spite of this rather complicated picture one can use relatively simple cage models to fit the re-orientational autocorrelation functions. This can even be done to fit CFs of different fragments, but the interpretation of the model parameters in this case can be rather speculative. Conversely, to model the re-orientation of the whole molecule one can use well-determined molecular parameters. For a more precise fit of the experimental functions one has to account for the distribution function of the cage potential curvature. Fast variations in the curvature strongly distort the short-time evolution of the CFs, making it impossible (and probably not necessary) to distinguish between different cage models (multiple cages or one diffusing cage).

Financial support of the Deutsche Forschungsgemeinschaft and NATO Science Committee, which enabled us to perform the computer simulations and collaborative work, is gratefully acknowledged. The authors are grateful to A. Ferrarini for fruitful discussions.

References

[1] Blinov, L. M., 1983, *Electro-Optical and Magneto-Optical Properties of Liquid Crystals* (New York: Wiley), Chap. 2.
[2] Luckhurst, G. R., and Veracini, C. A., 1994, *The Molecular Dynamics of Liquid Crystals* (Dordrecht: Kluwer).
[3] Deeg, F. W., Stankus, J. J., Greenfield, S. R., Newell, V. J., and Fayer, M. D., 1989, *J. chem. Phys.*, **90**, 6893.
[4] Foggi, P., Righini, R., Torre, R., and Kamalov, V. F., 1992, *Chem. Phys. Lett.*, **193**, 23.
[5] Ratchkevitch, V. S., Yakovenko, S. Ye., and Pelzl, J., 1993, *Liquid Crystals*, **15**, 591.
[6] Allen, M. P., and Tildesley, D. J., 1987, *Computer Simulation of Liquids* (Oxford: Clarendon Press).
[7] Yakovenko, S. Ye., Minko, A. A., Kroemer, G., and Geiger, A., 1994, *Liquid Crystals*, **17**, 127.
[8] van Gunsteren, W. F., and Berendsen, H. J. C., 1987, GROMOS: Groningen Molecular Simulation Software (University of Groningen).
[9] Nilsson, L., and Karplus, M., 1986, *J. Comput. Chem.*, **7**, 591.
[10] Kroemer, G., Paschek, D., and Geiger, A., 1993, *Ber. Bunsenges. Phys. Chem.*, **97**, 1188.
[11] Fontana, M. P., Rosi, B., Kirov, N., and Dozov, I., 1986, *Phys. Rev.* A, **33**, 4132.
[12] Zannoni, G., 1979, *Molec. Phys.*, **38**, 1813.
[13] Van Kampen, N. G., 1981, *Stochastic Processes in Physics and Chemistry* (Amsterdam: North-Holland), p. 13.
[14] Pasini, P., and Zannoni, C., 1984, *Molec. Phys.*, **52**, 749.
[15] Kivelson, D., and Keyes, T., 1972, *J. chem. Phys.*, **57**, 4599.
[16] Debye, P., 1929, *Polar Molecules* (New York: Dover).
[17] Gordon, R. G., 1966, *J. chem. Phys.*, **44**, 1830.
[18] Praestgraad, E., and Van Kampen, N. G., 1981, *Molec. Phys.*, **43**, 33.

[19] DOZOV, I., KIROV, N., and FONTANA, M. P., 1984, *J. chem. Phys.*, **81**, 2585.
[20] KIROV, N., DOZOV, I., and FONTANA, M. P., 1985, *J. chem. Phys.*, **83**, 5267.
[21] MORO, G., and NORDIO, P. L., 1983, *Chem. Phys. Lett.*, **96**, 192.
[22] MORO, G. J., NORDIO, P. L., NORO, M., POLIMENO, A., 1994, *J. chem. Phys.*, **101**, 693.
[23] MORO, G., and NORDIO, P. L., 1979, *Chem. Phys.*, **43**, 303.
[24] LASSIER, B., and BROT, C., 1969, *Discuss. Faraday Soc.*, **48**, 39.
[25] VARSHALOVICH, D. A., MOSKALEV, A. N., and KHERSONSKII, V. K., 1988, *Quantum Theory of Angular Momentum*, (Singapore: World Scientific), chaps 1–4.
[26] WYLLIE, G., 1971, *J. Phys.* C, **4**, 564.